

Lanthanide Luminescence Supramolecular Switch Based on Photoreactive Ammonium Molybdate

Ying Wu,[†] Lei Chen,[†] Yong Chen, and Yu Liu*Cite This: *ACS Appl. Mater. Interfaces* 2021, 13, 59126–59131

Read Online

ACCESS |



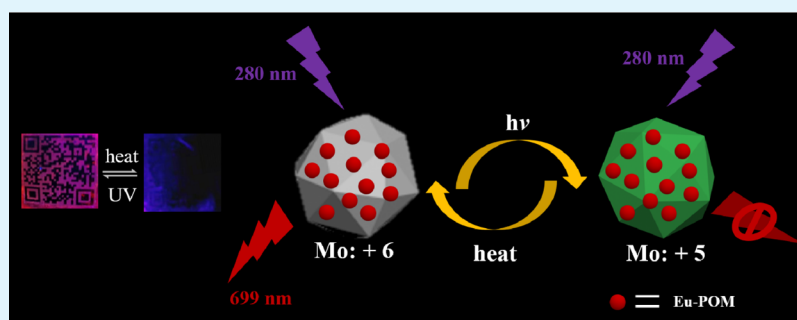
Metrics & More



Article Recommendations



Supporting Information



ABSTRACT: Lanthanide supramolecular assemblies as photoswitches have attracted much attention in the fields of cellular imaging and light-emitting materials. However, the regulation of lanthanide luminescence behavior by redox of metal ions is rare. Herein, we constructed a lanthanide luminescence supramolecular switch, that is, a binary assembly constructed by mono-(6-ethylenediamine-6-deoxy)- β -cyclodextrin (ECD) and ammonium molybdate tetrahydrate ($(\text{NH}_4)_6\text{Mo}_7\text{O}_{24}\cdot 4\text{H}_2\text{O}$, Mo_7), and further assembled into ternary assemblies with polyoxometalate $\text{Na}_9[\text{XW}_{10}\text{O}_{36}]\cdot 32\text{H}_2\text{O}$ (X-POM, X = Eu and Dy), which was comprehensively characterized by UV-vis, fluorescence, NMR, Fourier transform infrared, dynamic light scattering, scanning electron microscopy, and ζ potential. Thanks to the oxygen-shielding effect of secondary supramolecular assembly, the photoreduction process of Mo_7 (VI) could occur rapidly and efficiently. Due to the high Förster resonance energy transfer (FRET) efficiency of X-POM and Mo_7 (V) in supramolecular assembly, the photoreduction process is accompanied by fluorescence quenching. In addition, the oxidation process of the Mo_7 (V) could be rapidly promoted by heating, which allowed the X-POM fluorescence to recover. Interestingly, ECD-mediated ternary supramolecular assemblies not only tune the lanthanide luminescence but also strongly increase the lanthanide luminescence behavior, leading to the emission of strong narrow red light at ${}^5\text{D}_0$ - ${}^7\text{F}_4$, which can be successfully applied to two-dimensional code anticounterfeiting. In this study, a new approach is provided for the construction of lanthanide luminescence supramolecular switches tuned by photoreactive polyoxometalate.

KEYWORDS: lanthanide supramolecular assemblies, ammonium molybdate, β -cyclodextrin derivatives, supramolecular hydrogel, fluorescence switch

INTRODUCTION

Photochromic materials, including organic and inorganic materials,^{1–7} have attracted wide attention because of their efficient light-response rate and excellent fatigue resistance. For example, the commercially available ammonium molybdate tetrahydrate (Mo_7) with a proton-donating substance can undergo a Mo_7 (VI) to Mo_7 (V) photoreduction reaction under ultraviolet (UV) light but recover to Mo_7 (VI) under heating in the air,³⁴ and this conversion is accompanied by a colorless-to-green reversible change.⁸ This type of intelligent response group has been regarded as an ideal candidate for an anticounterfeiting material. Moreover, the process of the photoreduction reaction can be accelerated in deoxygenated solution, which greatly gives us inspiration that Mo_7 (VI) should be encapsulated in a suitable substrate to build a smart material. Generally, the suitable substrate matrix needs to meet

two conditions: (1) containing protons that can be captured by Mo_7 (VI) under UV light and (2) providing an environment that can effectively isolate oxygen under the air condition to promote photoreduction of Mo_7 (VI). Recently, Gao and co-workers reported Mo_7 (VI)-based photochromic films and rewritable papers.^{9,10} However, to the best of our knowledge, supramolecular fluorescence switches constructed by Mo_7 are rarely reported.

Received: October 4, 2021

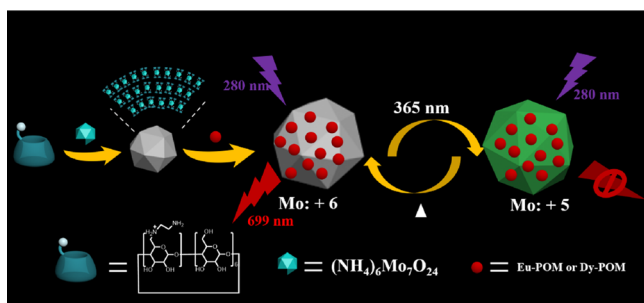
Accepted: November 24, 2021

Published: December 6, 2021



Supramolecular assembly, especially cyclodextrin-based supramolecular hybrid assembly constructed via noncovalent interaction, has significant advantages in the fabrication of multifunctional materials owing to good compatibility, availability, and ease of modification.^{11–17} For example, we constructed a negatively charged cyclodextrin assembly that induced excimer emission supramolecular assembly with photocontrolled energy transfer.¹⁸ Wu and co-workers reported an integrated catalyst consisting of cationic cyclodextrin, which is selective due to the cavity to screen the molecules in size.¹⁹ Zhao and co-workers constructed a cyclodextrin-modified nanoparticle photodynamic therapy (PDT) system that can improve nanoparticle stability and ensure high efficacy of PDT in hypoxia.²⁰ Herein, we constructed a reversible color switching material from the negatively charged polyoxometalate, ammonium molybdate tetrahydrate (Mo_7), and positively charged mono-(6-ethylenediamine-6-deoxy)- β -cyclodextrin (ECD) via electrostatic and hydrogenbond interactions. The inherent advantages of this hybrid assembly are as follows: (1) the electrostatic interactions between polycationic ECD and polyanionic Mo_7 are convenient to the formation of assembled nanostructures. (2) The supramolecular assembly constructed by ECD and Mo_7 has an oxygen-shielding effect and can promote the photochemical process of Mo_7 .^{15,21} The supramolecular construction strategy is relatively simple, which does not require complicated synthesis and separation compared with other reference methods. Furthermore, we utilized the host–guest interaction between adamantane-modified acrylamide (AdAm) and Mo_7 @ECD to form the AdAm- Mo_7 @ECD hydrogel. Interestingly, after the addition of Eu-POM and Dy-POM, the resultant system was endowed with photoswitchable red and white fluorescence, respectively (Scheme 1).

Scheme 1. Lanthanide Luminescence Supramolecular Switch Construction Process and Regulation of the Fluorescence Process



EXPERIMENTAL SECTION

Materials and Methods. All reagents were commercially available and used as supplied without further purification unless otherwise stated. All aqueous solutions were prepared in distilled water. NMR spectra were recorded on a Bruker AV400 instrument. UV–vis spectra were recorded on a Shimadzu UV-3600 spectrophotometer in a quartz cell (light path 10 mm) at 25 °C. Fluorescence emission spectra were recorded in a conventional quartz cell (10 × 10 × 45 mm) at 25 °C on a Varian Cary Eclipse equipped with a Varian Cary single-cell Peltier accessory to control temperature. Scanning electron microscopy (SEM) images were recorded on a JEOL JSM-7500F scanning electronic microscope operating at an accelerating voltage of 30 keV. The rheology test was performed on an AR 2000ex (TA Instrument) system, and 40 mm parallel plates were used during

the experiment at a gap of 1000 μm . Field-emission SEM images were characterized using a JEOL JSM-7500F with an accelerating voltage of 5.0 kV. Dynamic light scattering (DLS) measurements were performed on a laser light-scattering spectrometer (BI-200SM) equipped with a digital correlator (Turbo Corr.) at 636 nm at a scattering angle of 90°. Column chromatography was performed on 200–300 mesh silica gel. The light source used for the photoreaction was UV spotlight (5 W).

Synthesis of ECD. ECD was synthesized as described in the literature.^{22,23}

Synthesis of Adamantane Acrylamide (AdAm).^{23,24} Amantadine and triethylamine were dissolved in dry dichloromethane, and acryloyl chloride was added dropwise under the condition of ice bath and reacted at room temperature for 2 h.

Synthesis of X-POM (X = Eu and Dy). A total of 8.3 g of $\text{Na}_2\text{WO}_4 \cdot 2\text{H}_2\text{O}$ was dissolved in 20 mL of water; then, the pH of the solution was adjusted to 7.2 with CH_3COOH . A total of 1.1 g of $\text{Eu}(\text{NO}_3)_3$ in 2 mL of aqueous solution was added dropwise to the above-mentioned solution with stirring at 85 °C. The solution was cooled to room temperature, and the obtained crystals were filtered and dried to get a yield of 95%.⁸

Preparation of the AdAm Hydrogel.²⁵ Adamantane-modified acrylamide monomer (AdAm) (144 mg, 0.70 mmol), acrylamide (448 mg, 6.30 mmol), and N,N' -methylenebis (acrylamide) (MBA) (5.40 mg, 0.035 mmol) were dissolved in dimethyl sulfoxide (DMSO) (2 mL). Then, 1-hydroxycyclohexylphenylketone (HCH) (36.2 mg, 0.177 mmol) was added to the solution, and the mixture was irradiated under ultraviolet light for 2 h. Rectangle-shaped samples were washed successively with DMSO and deionized water.

Preparation of the AdAm-X-POM@ Mo_7 @ECD Hydrogel. The AdAm hydrogel was soaked in the 3.5 mmol/L X-POM@ Mo_7 @ECD aqueous solution for 24 h.

Preparation of the Two-Dimensional Code. The affirmative hydrogel is cut into a square with a length of 1 cm, then the two-dimensional code sticker with 0.8 cm length is glued to the surface of the hydrogel, and the pattern of the two-dimensional code is stuck to the gel surface.

RESULTS AND DISCUSSION

Ammonium molybdate tetrahydrate (Mo_7), as a polyanionic polyoxometalate with reversible photochromic property, has high water solubility and is hard to form a self-aggregate independently.^{26,27} ECD, synthesized according to the literature,²⁴ can be protonated under acidic conditions to form an assembly with negatively charged Mo_7 (pH = 5.5, Figures S1 and S2). Therefore, an obvious Tyndall effect was observed after mixing ECD and Mo_7 in aqueous solution, demonstrating the formation of large aggregates in solution.²⁸ In contrast, no obvious Tyndall phenomenon was observed in pure ECD or Mo_7 aqueous solution (Figure S3). To quantitatively determine the equivalence relationship between ECD and Mo_7 , the photochromic process of the binary assembly was monitored by UV–vis spectroscopy. As shown in Figure 1a, Mo_7 @ECD in aqueous solution with different molar ratios ($[\text{ECD}] + [\text{Mo}_7] = 7 \text{ mmol}$) showed obvious photochromism, in which the ratios of 5:2 and 6:1 were more effective. Moreover, SEM images showed that different proportions of Mo_7 and ECD solutions led to different morphologies of assembly (Figures 1b and S4). When the molar fraction of ECD and Mo_7 was 6:1, scattered nanoparticles with a diameter range of 80–120 nm were observed. Therefore, the preferable mixing ratio between ECD and Mo_7 was determined as 6:1.

DLS, ζ potential, and Fourier transform infrared (FT-IR) experiments were also performed to characterize the structural features of Mo_7 @ECD assembly. As seen in Figure 1c, the

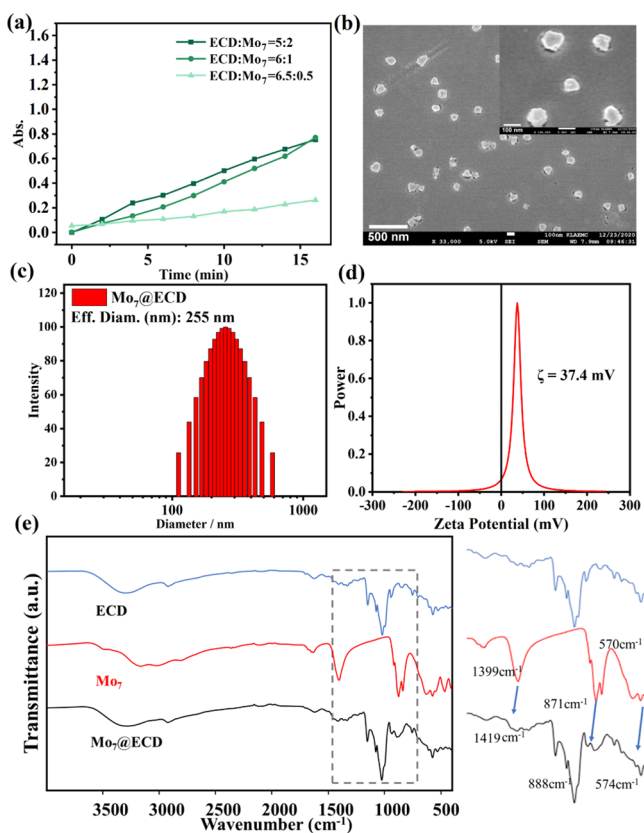


Figure 1. (a) UV absorption changes in Mo₇@ECD in aqueous solutions with different molar ratios at 25 °C under UV irradiation ([ECD] + [Mo₇] = 7 mM). (b) SEM image of the hybrid assembly constructed by ECD and Mo₇. (c) DLS data. [ECD] = 6 mM, [Mo₇] = 1 mM. (d) ζ potential of the assembly in aqueous solution at 25 °C. (e) FT-IR spectra of ECD, Mo₇, and Mo₇@ECD hybrid assembly.

average hydrodynamic diameter of Mo₇@ECD assembly was measured as about 255 nm by DLS, which was larger than the corresponding value measured by SEM, indicating the certain hydration of assembly in solution.²⁹ No appreciable DLS signals of free ECD or Mo₇ were observed. The ζ potential of nanoparticles was measured as $+37.4 \pm 1.05$ mV (Figure 1d), indicating that the Mo₇@ECD assembly was highly cationic. Consequently, we can infer that this assembly will have the capability of loading anionic substrates. In the FT-IR spectra (Figure 1e), Mo₇ showed three main characteristic peaks at 570 cm⁻¹ (Mo–O), 871 cm⁻¹ (Mo=O), and 1399 cm⁻¹ (Mo–O), demonstrating a Keggin structure of (NH₄)₆Mo₇O₂₄·4H₂O.³⁰ After association with ECD, the wavenumbers of Mo–O and Mo=O stretches shifted to 574, 888, and 1419 cm⁻¹, respectively, indicating the strong electrostatic interactions between ECD and Mo₇. Moreover, the appearance of a new band at 704 cm⁻¹ also indicated the formation of a hydrogen bond between the O atoms of Mo–O and the protons on amino groups. These results indicate that Mo₇ and ECD formed a hybrid structure, where the Keggin structure of Mo₇ still remained. According to the references and combined with SEM images,^{29,31,32} a possible formation mechanism of this hybrid structure may explain the formation of nanoparticles. The free Mo₇ could not form large self-aggregates. When ECD was added, various Mo₇ and ECD combined with each other via hydrogen bond and electrostatic interactions to form large layer-by-layer aggregates that

subsequently bended to layer-by-layer nanoparticles with alternating shell structures. In addition, the Mo₇@ECD assembly presented the good stability because its UV–vis absorbance showed no obvious changes for at least 2 h at room temperature (Figure S5).

In order to explore the role of ECD in photoreduction, different substrates were selected as control groups to observe photochromism, including ethylenediamine, glucosamine, acrylamide, and ethylene glycol. Naked eyes and UV–vis spectroscopy were used to monitor the photochromic process. After mixing 1 mM Mo₇ and 6 mM ECD, the change in UV–vis absorbance was measured every 2 min. As shown in Figure 2a,b, with the continuous increase in irradiation time, the

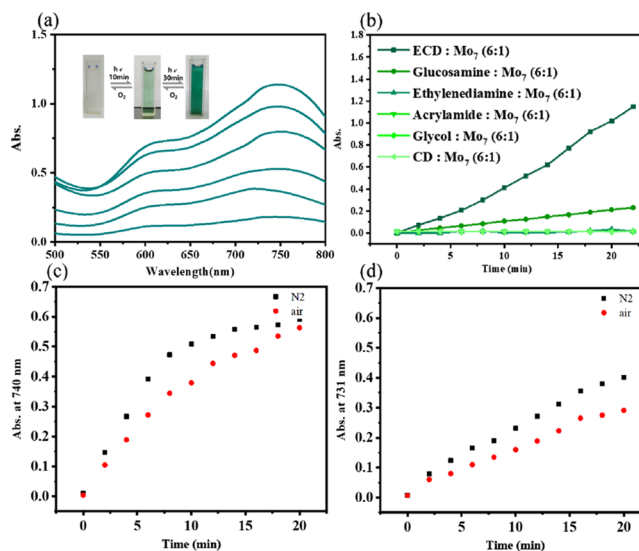


Figure 2. (a) Change in UV absorption of Mo₇@ECD with the increase in illumination time (the wavelength of UV lamp = 365 nm). (b) Optical absorption of various positive donor proton compounds and negative Mo₇ in aqueous solutions with different molar ratios at 25 °C. [substances] + [Mo₇] = 7 mM, Absorption at 740 nm, pH = 5.5. Substances are β -cyclodextrin, ethylenediamine, glucosamine, acrylamide, and ethylene glycol. The change in UV absorption of (c) Mo₇@ECD and (d) glucosamine-Mo₇ in aqueous solutions in nitrogen and air at 25 °C, respectively. [ECD] = [glucosamine] = 6 mM, [Mo₇] = 1 mM.

intensity of the UV–vis absorption peak of Mo₇@ECD increased at 550–800 nm, which showed a fast photochromic rate. Equal proportion of glucosamine-Mo₇ showed a slow photochromic rate (Figures 2b and S6). No obvious sign of photochromism in the other control groups (Figure S7) was observed. Therefore, we deduce that the formation of supramolecular assemblies between ECD and Mo₇ via electrostatic interaction is an important prerequisite for the generation of efficient photochromes.

To explore the possible mechanism of the photochromism in Mo₇@ECD, the assembly solution was irradiated at 365 nm for 20 min in nitrogen and in the air, respectively. The results showed that the absorbance of Mo₇@ECD tended to be the same. In the control experiment, the absorbance of glucosamine-Mo₇ reached 0.289 and 0.410 in air and nitrogen separately, indicating that the oxygen in the air hindered the photoreduction process and inhibited the proton transfer between H on the amino group and O on Mo–O (Figure 2c,d). In addition, the UV–vis absorbance of Mo₇ has no

obvious change whatever be it in nitrogen or in the air under the UV irradiation (Figure S7). Therefore, we can deduce that the Mo₇@ECD assembly can effectively hinder the external oxygen. In the air, the discoloration processes of Mo₇@ECD took 12 h but greatly shortened to 10 min under heating at 80 °C (Figure S8). A possible reason may be as follows. During the discoloration, the steric hindrance from the cavity of cyclodextrin made it difficult for oxygen to contact with Mo₇ and the amino group of ECD; thus, the oxidation process was difficult to some extent, but the heating could greatly accelerate the movement of oxygen and thus shorten the discoloration process. Figure S9 depicts a transfer of a proton from a hydrogen-bonded ECD to Mo₇'s O–Mo during the photo-reduction process, and the oxidation process was its inverse process.³³

Na₉[XW₁₀O₃₆]·32H₂O (X-POM, X = Eu and Dy) was prepared according to the previous reports.^{8,34} As shown in Figure 3a, the discrete Eu-POM solution displayed obvious

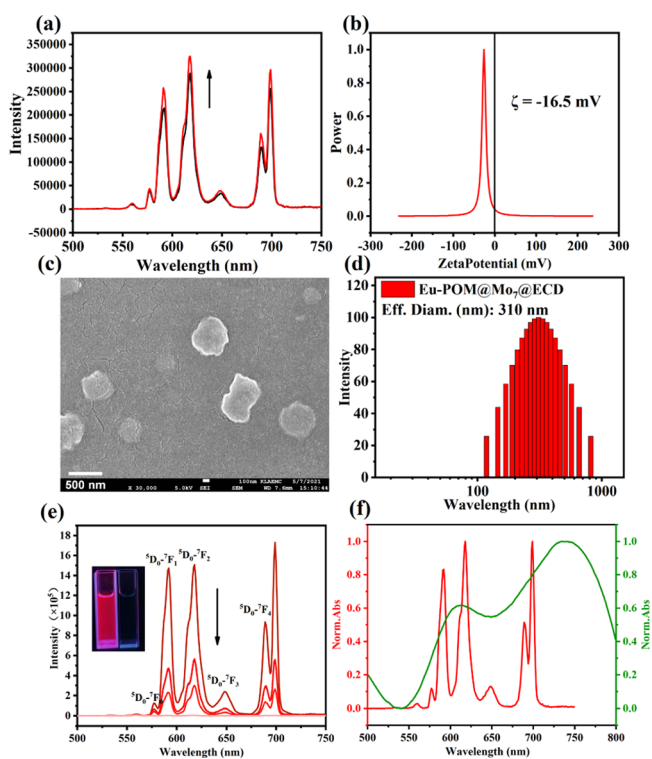


Figure 3. (a) Fluorescence intensity of Eu-POM increased with the addition of Mo₇@ECD. (b) ζ potential of Eu-POM@Mo₇@ECD in aqueous solution at 25 °C; (c) SEM images; (d) DLS data. (e) Fluorescence spectra of Eu-POM and Mo₇@ECD with the increase in illumination time ($\lambda_{\text{ex}} = 280$ nm). The concentration of Eu-POM was fixed at 5×10^{-6} M, and the concentration Mo₇@ECD is 0.02 times that of Eu-POM. The illumination time increases from 0 to 25 min (f) UV absorption and fluorescence emission after normalization.

characteristic transitions of Eu³⁺ when irradiated at 280 nm, mainly owing to the intramolecular energy transfer from the ligand-to-metal charge transfer band of O/W to the photoluminescent Eu³⁺ core.^{8,35} When the ECD was added to the Eu-POM solution, the fluorescence intensity of Eu-POM increased (Figure 3a), illustrating that Eu-POM and ECD existed electrostatic interaction.⁶ The ζ potential of nanoparticles was measured as -16.5 mV (Figure 3b). The average diameter of Eu-POM@Mo₇@ECD was measured as about

150–200 nm (Figure 3c,d), which was larger than that of the Mo₇@ECD. These properties jointly indicated that the Eu-POM@Mo₇@ECD supramolecular assembly was formed. Interestingly, with the occurrence of Mo₇@ECD photo-reduction, the color of the solution changed from colorless to green in the bright field, accompanied by the quenching of Eu-POM@Mo₇@ECD fluorescence (Figure 3e), which could be recovered by heating (Figure S10). A similar phenomenon was also observed in the Dy-POM@Mo₇@ECD complex. These phenomena could be attributed to the fact that the absorption band of the photoreduction Mo₇@ECD well-overlapped with the fluorescence emission of the X-POM, which was favorable for the Förster resonance energy transfer (FRET) process (Figures 3f and S11), and the energy-transfer efficiency (Φ_{ET}) was calculated as 94% in aqueous solution (Figure S10).

Subsequently, a hydrogel with AdAm was successfully prepared (Figures S12 and S13).^{23,25,36} A well-swollen and highly transparent hydrogel AdAm-Eu-POM@Mo₇@ECD was obtained when AdAm was immersed in the aqueous solution of Eu-POM@Mo₇@ECD (Figures S14–S16). The response to external stimuli is a significant property of this hydrogel. An on–off switch of the fluorescence of AdAm-Eu-POM@Mo₇@ECD based on a photoreaction in Mo₇@ECD was observed. The two-dimensional code was pasted on the hydrogel,^{37,38} code on the photoreduction X-POM@Mo₇@ECD was invisible and became visible on the oxidized X-POM@Mo₇@ECD under a commercial portable UV lamp (254 nm) (Figure 4), allowing for readout of the stored information. Then, we tried to erase the pattern with 365 nm light.

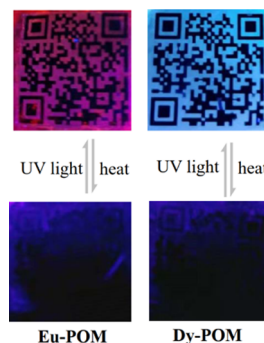


Figure 4. Photographs of Eu-POM and Dy-POM, respectively, with a supramolecular hydrogel before and after 365 nm UV irradiation and its reversible process under an oxygen environment.

After irradiation, the luminescence of the X-POM@Mo₇@ECD hydrogel was quenched and the pattern could not be read out anymore under the UV lamp. Interestingly, the quenched hydrogel could gradually recover upon heating at 80 °C (Figure 4), and the code could be observed again. Moreover, the photocontrolled erase/recover cycles could be repeated (Video V1 in the Supporting Information). The redox process of the assembly can be used as a fluorescent switch for different lanthanide-POM@Mo₇@ECD. These properties jointly indicated an application potential of assembly as photochromic optical memory and data storage materials.

CONCLUSIONS

In conclusion, we have successfully constructed tunable lanthanide fluorescent switch supramolecular assembly through

electrostatic interaction between X-POM, Mo₇, and ECD. The photoreduction process of Mo₇(VI) could rapidly and efficiently occur due to the oxygen-shielding effect in Mo₇@ECD supramolecular assembly. Interestingly, due to the high FRET efficiency of X-POM and Mo₇(V) in supramolecular assembly, the fluorescence of X-POM in X-POM@Mo₇@ECD is regulated by controlling the redox state of Mo₇. Significantly, taking advantage of the characteristics of supramolecular assembly, the two-dimensional code of encoded information can be encrypted and decrypted under UV light and heating conditions. This smart fluorescent switch constructed by the supramolecular concept provides a development path in the fields of intelligent response lanthanide luminescent materials.

■ ASSOCIATED CONTENT

SI Supporting Information

The Supporting Information is available free of charge at <https://pubs.acs.org/doi/10.1021/acsami.1c19076>.

Reagents and materials, methods and characterizations, fabrication of the supramolecular hydrogel, photochromic process of Mo₇@ECD, fluorescence spectra, SEM images, ¹H NMR and 2D ROESY NMR, and rheological characterization of AdAm with ECD and POM hydrogels (PDF)

Process of fluorescence changes in the supramolecular hydrogel (MP4)

■ AUTHOR INFORMATION

Corresponding Author

Yu Liu – College of Chemistry, State Key Laboratory of Elemento-Organic Chemistry, Nankai University, Tianjin 300071, P. R. China; orcid.org/0000-0001-8723-1896; Email: yuliu@nankai.edu.cn

Authors

Ying Wu – College of Chemistry, State Key Laboratory of Elemento-Organic Chemistry, Nankai University, Tianjin 300071, P. R. China

Lei Chen – College of Chemistry, State Key Laboratory of Elemento-Organic Chemistry, Nankai University, Tianjin 300071, P. R. China

Yong Chen – College of Chemistry, State Key Laboratory of Elemento-Organic Chemistry, Nankai University, Tianjin 300071, P. R. China

Complete contact information is available at: <https://pubs.acs.org/doi/10.1021/acsami.1c19076>

Author Contributions

[†]Y.W. and L.C. contributed equally to this work.

Funding

This work was financially supported by the National Natural Science Foundation of China (grant nos. 22131008 and 21971127).

Notes

The authors declare no competing financial interest.

■ ACKNOWLEDGMENTS

We thank the National Natural Science Foundation of China (NNSFC) (grant nos. 22131008 and 21971127) for financial support.

■ REFERENCES

- (1) Ji, X.; Shi, B.; Wang, H.; Xia, D.; Jie, K.; Wu, Z. L.; Huang, F. Supramolecular Construction of Multifluorescent Gels: Interfacial Assembly of Discrete Fluorescent Gels through Multiple Hydrogen Bonding. *Adv. Mater.* **2015**, *27*, 8062–8066.
- (2) Wu, H.; Chen, Y.; Dai, X.; Li, P.; Stoddart, J. F.; Liu, Y. In Situ Photoconversion of Multicolor Luminescence and Pure White Light Emission Based on Carbon Dot-Supported Supramolecular Assembly. *J. Am. Chem. Soc.* **2019**, *141*, 6583–6591.
- (3) Yao, J. N.; Hashimoto, K.; Fujishima, A. Photochromism Induced in an Electrolytically Pretreated MoO₃ thin Film by Visible Light. *Nature* **1992**, *355*, 624–626.
- (4) Peng, Z. Rational Synthesis of Covalently Bonded Organic-Inorganic Hybrids. *Angew. Chem., Int. Ed.* **2004**, *43*, 930–935.
- (5) Yang, Z.; Du, J.; Martin, L. I. D. J.; van der Heggen, D.; Poelman, D. Highly Responsive Photochromic Ceramics for High-Contrast Rewritable Information Displays. *Laser Photonics Rev.* **2021**, *15*, 2000525.
- (6) Zhang, J.; Liu, Y.; Li, Y.; Zhao, H.; Wan, X. Hybrid Assemblies of Eu-Containing Polyoxometalates and Hydrophilic Block Copolymers with Enhanced Emission in Aqueous Solution. *Angew. Chem., Int. Ed.* **2012**, *51*, 4598–4602.
- (7) Chen, X.-M.; Hou, X.-F.; Bisoyi, H. K.; Feng, W.-J.; Cao, Q.; Huang, S.; Yang, H.; Chen, D.; Li, Q. Light-fueled transient supramolecular assemblies in water as fluorescence modulators. *Nat. Commun.* **2021**, *12*, 4993.
- (8) Sugeta, M.; Yamase, T. Crystal Structure and Luminescence Site of Na₉[EuW₁₀O₃₆]·32H₂O. *Bull. Chem. Soc. Jpn.* **1993**, *66*, 444–449.
- (9) Yang, Y.; Guan, L.; Gao, G. Low-Cost, Rapidly Responsive, Controllable, and Reversible Photochromic Hydrogel for Display and Storage. *ACS Appl. Mater. Interfaces* **2018**, *10*, 13975–13984.
- (10) Yang, Y.; Xu, J.; Li, Y.; Gao, G. Gelatin/PVA Compositing Photochromic Film for Light Printing with Fast Rewritability and Long-Term Storage Ability. *J. Mater. Chem. C* **2019**, *7*, 12518–12522.
- (11) Schmidt, B. V. K. J.; Barner-Kowollik, C. Dynamic Macromolecular Material Design-The Versatility of Cyclodextrin-Based Host-Guest Chemistry. *Angew. Chem., Int. Ed.* **2017**, *56*, 8350–8369.
- (12) Yu, G.; Zhao, X.; Zhou, J.; Mao, Z.; Huang, X.; Wang, Z.; Hua, B.; Liu, Y.; Zhang, F.; He, Z.; Jacobson, O.; Gao, C.; Wang, W.; Yu, C.; Zhu, X.; Huang, F.; Chen, X. Supramolecular Polymer-Based Nanomedicine: High Therapeutic Performance and Negligible Long-Term Immunotoxicity. *J. Am. Chem. Soc.* **2018**, *140*, 8005–8019.
- (13) Loebel, C.; Rodell, C. B.; Chen, M. H.; Burdick, J. A. Shear-Thinning and Self-Healing Hydrogels as Injectable Therapeutics and for 3D-Printing. *Nat. Protoc.* **2017**, *12*, 1521–1541.
- (14) Chen, L.; Chen, Y.; Fu, H. G.; Liu, Y. Reversible Emitting Anti-Counterfeiting Ink Prepared by Anthraquinone-Modified beta-Cyclodextrin Supramolecular Polymer. *Adv. Sci.* **2020**, *7*, 2000803.
- (15) Zhang, G.; Li, B.; Zhou, Y.; Chen, X.; Li, B.; Lu, Z.-Y.; Wu, L. Processing Supramolecular Framework for Free Interconvertible Liquid Separation. *Nat. Commun.* **2020**, *11*, 425.
- (16) Liu, Z.; Dai, X.; Sun, Y.; Liu, Y. Organic Supramolecular Aggregates based on Water-Soluble Cyclodextrins and Calixarenes. *Aggregate* **2020**, *1*, 31–44.
- (17) Wang, Q.; Zhang, Q.; Zhang, Q.-W.; Li, X.; Zhao, C.-X.; Xu, T.-Y.; Qu, D.-H.; Tian, H. Color-Tunable Single-Fluorophore Supramolecular System with Assembly-Encoded Emission. *Nat. Commun.* **2020**, *11*, 158.
- (18) Li, J. J.; Zhang, H. Y.; Liu, G.; Dai, X.; Chen, L.; Liu, Y. Photocontrolled Light-Harvesting Supramolecular Assembly Based on Aggregation-Induced Excimer Emission. *Adv. Opt. Mater.* **2021**, *9*, 2001702.
- (19) Chen, X.; Zhang, G.; Li, B.; Wu, L. An Integrated Giant Polyoxometalate Complex for Photothermally Enhanced Catalytic Oxidation. *Sci. Adv.* **2021**, *7*, No. eabf8413.
- (20) Phua, S. Z. F.; Yang, G.; Lim, W. Q.; Verma, A.; Chen, H.; Thanabalu, T.; Zhao, Y. Catalase-Integrated Hyaluronic Acid as Nanocarriers for Enhanced Photodynamic Therapy in Solid Tumor. *ACS Nano* **2019**, *13*, 4742–4751.

(21) Zhou, Y.; Zhang, H.-Y.; Zhang, Z.-Y.; Liu, Y. Tunable Luminescent Lanthanide Supramolecular Assembly Based on Photo-reaction of Anthracene. *J. Am. Chem. Soc.* **2017**, *139*, 7168–7171.

(22) Nelles, G.; Weisser, M.; Back, R.; Wohlfart, P.; Wenz, G.; Mittler-Neher, S. Controlled Orientation of Cyclodextrin Derivatives Immobilized on Gold Surfaces. *J. Am. Chem. Soc.* **1996**, *118*, 5039–5046.

(23) Kretschmann, O.; Choi, S. W.; Miyauchi, M.; Tomatsu, I.; Harada, A.; Ritter, H. Switchable Hydrogels Obtained by Supramolecular Cross-Linking of Adamantyl-Containing LCST Copolymers with Cyclodextrin Dimers. *Angew. Chem., Int. Ed.* **2006**, *45*, 4361–4365.

(24) Ang, C. Y.; Tan, S. Y.; Wang, X.; Zhang, Q.; Khan, M.; Bai, L.; Tamil Selvan, S.; Ma, X.; Zhu, L.; Nguyen, K. T.; Tan, N. S.; Zhao, Y. Supramolecular Nanoparticle Carriers Self-Assembled from Cyclodextrin- and Adamantane-Functionalized Polyacrylates for Tumor-Targeted Drug Delivery. *J. Mater. Chem. B* **2014**, *2*, 1879–1890.

(25) Wang, S.; Xu, Z.; Wang, T.; Xiao, T.; Hu, X.-Y.; Shen, Y.-Z.; Wang, L. Warm/cool-tone Switchable Thermochromic Material for Smart Windows by Orthogonally Integrating Properties of Pillar[6]arene and Ferrocene. *Nat. Commun.* **2018**, *9*, 1737.

(26) Wales, D. J.; Cao, Q.; Kastner, K.; Karjalainen, E.; Newton, G. N.; Sans, V. 3D-Printable Photochromic Molecular Materials for Reversible Information Storage. *Adv. Mater.* **2018**, *30*, 1800159.

(27) Xu, J.; Volfova, H.; Mulder, R. J.; Goerigk, L.; Bryant, G.; Riedle, E.; Ritchie, C. Visible-Light-Driven “On”/“Off” Photochromism of a Polyoxometalate Diarylethene Coordination Complex. *J. Am. Chem. Soc.* **2018**, *140*, 10482–10487.

(28) Yan, X.; Zhu, P.; Fei, J.; Li, J. Self-Assembly of Peptide-Inorganic Hybrid Spheres for Adaptive Encapsulation of Guests. *Adv. Mater.* **2010**, *22*, 1283–1287.

(29) Wang, J.; Chen, Y.; Cheng, N.; Feng, L.; Gu, B.-H.; Liu, Y. Multivalent Supramolecular Self-Assembly between β -Cyclodextrin Derivatives and Polyoxometalate for Photodegradation of Dyes and Antibiotics. *ACS Appl. Bio Mater.* **2019**, *2*, 5898–5904.

(30) Li, C.; Xin, Q.; Wang, K.-L.; Guo, X. FT-IR Emission Spectroscopy Studies of Molybdenum Oxide and Supported Molybdena on Alumina, Silica, Zirconia, and Titania. *Appl. Spectrosc.* **1991**, *45*, 874–882.

(31) Jiao, J.; Sun, G.; Zhang, J.; Lin, C.; Jiang, J.; Wang, L. The Preparation of a Water-Soluble Phospholate-Based Macrocycle for Constructing Artificial Light-Harvesting Systems. *Chem. Eur. J.* **2021**, *27*, 16601–16605, DOI: 10.1002/chem.202102758.

(32) Li, J.-J.; Chen, Y.; Yu, J.; Cheng, N.; Liu, Y. A Supramolecular Artificial Light-Harvesting System with an Ultrahigh Antenna Effect. *Adv. Mater.* **2017**, *29*, 1701905.

(33) Yamase, T. Photo- and Electrochromism of Polyoxometalates and Related Materials. *Chem. Rev.* **1998**, *98*, 307–326.

(34) AlDamen, M. A.; Cardona-Serra, S.; Clemente-Juan, J. M.; Coronado, E.; Gaita-Ariño, A.; Martí-Gastaldo, C.; Luis, F.; Montero, O. Mononuclear Lanthanide Single Molecule Magnets Based on the Polyoxometalates $\text{Ln}(\text{W}_5\text{O}_{18})_2^{9-}$ and $\text{Ln}(\beta\text{-SiW}_{11}\text{O}_{39})_2^{13-}$ ($\text{Ln}(\text{III}) = \text{Tb}, \text{Dy}, \text{Ho}, \text{Er}, \text{Tm}, \text{and Yb}$). *Inorg. Chem.* **2009**, *48*, 3467–3479.

(35) Guo, Y.; Gong, Y.; Gao, Y. a.; Xiao, J.; Wang, T.; Yu, L. Multi-Stimuli Responsive Supramolecular Structures Based on Azobenzene Surfactant-Encapsulated Polyoxometalate. *Langmuir* **2016**, *32*, 9293–9300.

(36) Wang, S.; Gao, W.; Hu, X.-Y.; Shen, Y.-Z.; Wang, L. Supramolecular Strategy for Smart Windows. *Chem. Commun.* **2019**, *55*, 4137–4149.

(37) Li, Z.; Wang, G.; Ye, Y.; Li, B.; Li, H.; Chen, B. Loading Photochromic Molecules into a Luminescent Metal-Organic Framework for Information Anticounterfeiting. *Angew. Chem., Int. Ed.* **2019**, *58*, 18025–18031.

(38) Li, Z.; Liu, X.; Wang, G.; Li, B.; Chen, H.; Li, H.; Zhao, Y. Photoresponsive Supramolecular Coordination Polyelectrolyte as Smart Anticounterfeiting Inks. *Nat. Commun.* **2021**, *12*, 1363.